



PCCP

Effect of Impurities on Radical Formation in Gibbsite Radiolysis

Journal:	<i>Physical Chemistry Chemical Physics</i>
Manuscript ID	CP-COM-12-2023-006305.R1
Article Type:	Communication
Date Submitted by the Author:	20-Feb-2024
Complete List of Authors:	Hlushko, Hanna; University of Notre Dame, Radiation Laboratory Ramos-Ballesteros, Alejandro; University of Notre Dame Chen, Ping; Pacific Northwest National Laboratory Zhang, Xin; Pacific Northwest National Laboratory Rosso, Kevin; Pacific Northwest National Laboratory, Physical Sciences Division Pearce, Carolyn; Pacific Northwest National Laboratory, LaVerne, Jay; University of Notre Dame, Radiation Laboratory and Department of Physics and Astronomy

SCHOLARONE™
Manuscripts

COMMUNICATION

Effect of Impurities on Radical Formation in Gibbsite Radiolysis

Hanna Hlushko,^a Alejandro Ramos-Ballesteros,^a Ping Chen,^b Xin Zhang,^b Kevin M. Rosso,^b Carolyn I. Pearce,^{b,c} and Jay A. LaVerne^{*a,d}Received 00th January 20xx,
Accepted 00th January 20xx

DOI: 10.1039/x0xx00000x

The generation and stabilization of gamma radiation-induced hydrogen atoms in gibbsite ($\text{Al}(\text{OH})_3$) nanoplates is directly related to the nature of residual ions from synthetic precursors used, whether nitrates or chlorides. The concentration of hydrogen atoms trapped in the interstitial layers of gibbsite is lower and decays faster in comparison to boehmite (AlOOH), which could affect the waste management of these materials.

Aluminum was widely used as fuel cladding material for plutonium production at the U.S. Department of Energy's Hanford site (WA).^{1,2} The waste from fuel processing, including aluminium dissolved in sodium hydroxide, was disposed in underground tanks. Aluminium is present as solid oxyhydroxides such as boehmite ($\gamma\text{-AlOOH}$) and hydroxides such as gibbsite ($\gamma\text{-Al}(\text{OH})_3$), which represent a significant percent of mineral phases identified in Hanford legacy waste.^{2,3} The waste is a complex multicomponent chemical mixture that has been exposed to radiation, mostly beta-particles and gamma-rays from strontium-90 and cesium-137, for decades. This extreme environment has led to changes in speciation and reactivity that need to be understood to facilitate safe waste storage, retrieval, and processing. Additionally, the study of aluminum oxides as radiolytic substrates for hydrogen production⁴ is of paramount interest for the security and decarbonization of the energy sector. This paper focuses on comparing the nature and extent of radiolytic species formed from irradiation of gibbsite synthesized using different precursors, and from irradiation of boehmite, which is known to

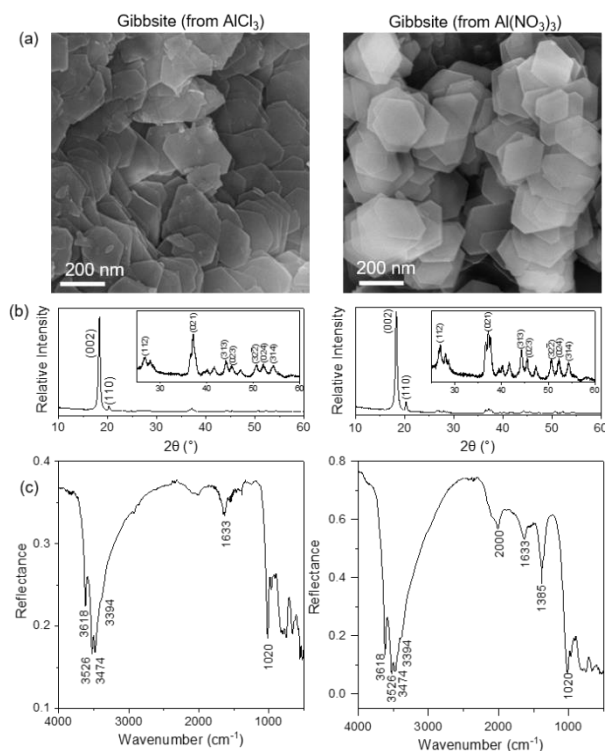


Figure 1. (a) SEM images, (b) pXRD patterns, and (c) DRIFTS spectra of gibbsite synthesized from AlCl_3 (left) and $\text{Al}(\text{NO}_3)_3$ (right).

trap and stabilize hydrogen (H) atoms.^{5,6} Interestingly, stable H atoms were also observed in the radiolysis of talc.⁷ No significant H atom formation was observed in previous radiolytic studies of gibbsite,⁸ or its polymorph bayerite ($\beta\text{-Al}(\text{OH})_3$).⁹ This difference in H atom observations between boehmite and gibbsite has been discussed in terms of H atom diffusion,¹⁰ but there is a lack of other experimental evidence. The precursors used to synthesize gibbsite can remain as impurities in the final product, which can affect the kinetics of H atom formation and trapping.

In this study, gibbsite particles were synthesized using a hydrothermal method,¹¹ as described in Supporting Information

^a Radiation Laboratory, University of Notre Dame, Notre Dame, 46556

^b Pacific Northwest National Laboratory, Richland, WA, 99354

^c Washington State University, Pullman, WA, 99163

^d Department of Physics and Astronomy, University of Notre Dame, Notre Dame, IN, 46556

† Corresponding author – Jay LaVerne, jay.a.laverne.1@nd.edu

Electronic Supplementary Information (ESI) available: [X-ray photoelectron spectroscopy spectra of gibbsites, Thermogravimetric analysis of the materials]. See DOI: 10.1039/x0xx00000x

(SI), using aluminum nitrate ($\text{Al}(\text{NO}_3)_3$) or aluminum chloride (AlCl_3) as a precursor. Both syntheses resulted in gibbsite nanoplatelets with similar average size (200–400 nm) (Fig. 1a) and powder X-ray diffraction (pXRD) patterns (Fig. 1b). The pXRD patterns and the distance between layers ($4.85 \pm 0.02 \text{ \AA}$)

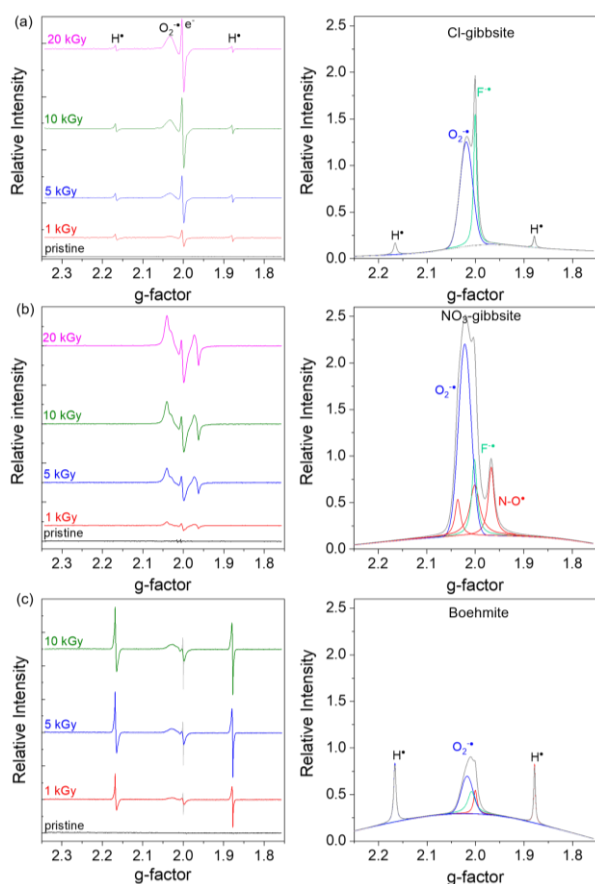


Figure 2. EPR spectra (left) and integrated and deconvoluted EPR spectra (right) of gibbsite synthesized from (a) AlCl_3 (top) or (b) $\text{Al}(\text{NO}_3)_3$, and (c) boehmite.

within the layered structure of gibbsite, calculated from the position of the first peak in pXRD, agrees well with that reported in the literature.¹²

Diffuse reflectance infrared Fourier transform spectroscopy (DRIFTS) revealed strong stretching vibrations of structural hydroxyl groups in gibbsite synthesized from both precursors, with the strongest bands at 3618, 3526, 3474, and 3394 cm^{-1} (Fig. 1c). Such distinctive features in the hydroxyl region are attributed to the difference in vibrations of all -OH groups in one repeating unit.¹³ The spectrum also revealed a strong peak at 1385 cm^{-1} in gibbsite synthesized from $\text{Al}(\text{NO}_3)_3$ (NO_3 -gibbsite) which corresponds to asymmetric NO_3^- vibration.¹⁴ This observation confirms the presence of residual nitrate at a concentration of ~ 0.4 atom percent, as estimated with X-ray photoelectron spectroscopy (XPS) (Fig. S1). In contrast, DRIFTS of the gibbsite synthesized from AlCl_3 (Cl-gibbsite) did not have a peak at 1385 cm^{-1} corresponding to NO_3^- , and XPS confirmed the presence of no detectable nitrogen, but revealed residual chloride (~ 0.6 atom percent) (Fig. S2). Nucleation to the solid may allow inclusion of some ions from the solution through electrostatic interactions and cannot be fully removed during

the subsequent washing procedure. The concentration of residual ions is too small to affect the bulk properties of gibbsite, but can still significantly affect the response of the material to radiolysis.

During radiolysis, surface water and surface hydroxyls are involved in the generation of radiolysis products.¹⁵ Thus, solid powders containing only surface water were irradiated in this work. Briefly, known amounts ($\sim 50 \text{ mg}$) of the gibbsite powders were sealed under vacuum in Suprasil® tubes and irradiated with a ^{60}Co - γ source at an approximate dose rate of 55 Gy/min, until the samples accumulated 1, 5, 10, or 20 kGy of absorbed dose. Radical formation and associated radical decay were studied with electron paramagnetic resonance (EPR) spectroscopy, as described in SI.

At all studied doses, the EPR spectra of Cl-gibbsite had four distinct peaks, including three sharp peaks ($g_1 = 2.1657$, $\text{FWHM}_1 = 0.00695$, $g_3 = 2.001$, $\text{FWHM}_3 = 0.00702$, and $g_4 = 1.8785$, $\text{FWHM}_4 = 0.00572$), and one broad peak ($g_2 = 2.0188$, $\text{FWHM}_2 = 0.0308$). Two of the sharp peaks ($g_1 = 2.1657$ and $g_4 = 1.8785$) with a hyperfine splitting constant $A = 1409.1 \text{ MHz}$ (49.78 mT) can be assigned to the H atom. The broad peak agrees with the literature and can be attributed to the $\text{O}-\text{O}^\bullet$ radical, which is in a symmetrical environment (isotropic).¹⁶ The other sharp peak ($g_3 = 2.001$) was previously detected in gibbsite, but was not assigned.¹⁶ It could be the O_3^\bullet radical or trapped electrons. These two oxygen-radical species were also detected in NO_3 -gibbsite, in agreement with published spectra.⁸ The results suggest that the formation of these oxygen-centred species occurs on the hydroxyl groups of gibbsite. No hydrogen peaks were observed in NO_3 -gibbsite, and in addition to the oxygen-centred radicals, this gibbsite had a well-defined triplet peak ($g_5 = 1.9676$, $\text{FWHM}_5 = 0.0143$, $g_6 = 2.0016$, $\text{FWHM}_6 = 0.0129$, and $g_7 = 2.0356$, $\text{FWHM}_7 = 0.0136$). Observation of the radical decay confirmed that the triplet ($A = 6 \text{ mT}$) belongs to another paramagnetic species, and it was assigned to the $\text{N}-\text{O}^\bullet$ radical in the vicinity of O_2^- . These results demonstrate that the presence of residual NO_3^- affects the observation of H atoms, possibly due to scavenging of the H atoms themselves or their precursors, or the modification of trapping sites. Irradiation of the Cl-gibbsite resulted in the formation of trapped H-atoms, but did not produce any stable and detectable Cl radicals. Kaddissy et al. first proposed that H atoms are formed by breaking the O-H bond,⁹ and calculations have suggested that this mechanism is responsible for H atom formation in both gibbsite and boehmite followed by recombination of H atoms.¹⁰ It can be assumed that H atoms are formed in both cases but are only trapped in the absence of NO_3^- ; further experiments will verify this.

EPR spectroscopy was used to further explore how aluminum hydroxide/oxyhydroxide structure affects radiolytic H atom production and stabilization.¹⁶ The boehmite used by Huestis et al. (2020) was commercially produced, and the platelets were 0.5 to 1 μm across with a thickness of approximately 200 nm (Fig. S3). The commercially produced boehmite did not appear to contain any impurities from the precursor materials. Fig. 2c shows the intensities of H atom peaks in boehmite are greater than that of the oxygen-centred radicals in contrast with

gibbsite, where oxygen-centered species dominate the spectrum. The shape of the spectra agrees with the literature.⁵ Interestingly, the hyperfine splitting ($A = 1410.2$ MHz or 49.82 mT) for boehmite is the same as for gibbsite, suggesting that H atoms in both materials have similar environments. In boehmite, three principal components of $O_2^{\cdot-}$ ($g_x=2.017$,

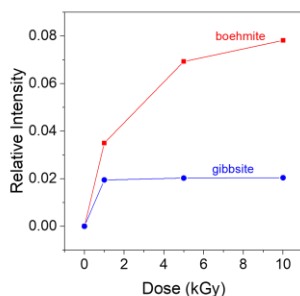


Figure 3. Dependence of integrated H atom peak intensity on radiation dose for (■) boehmite and (●) Cl-gibbsite.

$g_y=2.007$, and $g_z=2.000$) were easily observed, confirming rhombic geometry of the paramagnetic center.¹⁷ Even though removing the NO_3^- impurity by using a Cl^- precursor in the gibbsite synthesis resulted in the formation of trapped H atoms, the number of these radicals was relatively small compared with boehmite irradiated to the same dose. While the intensity of H atoms in the boehmite spectra gradually increased with the dose, reaching the plateau at ~ 20 kGy (Fig. 3), the intensity of H atoms in Cl-gibbsite maximized at 1 kGy and stayed at the same level up to 10 kGy of adsorbed dose. This result is indicative of

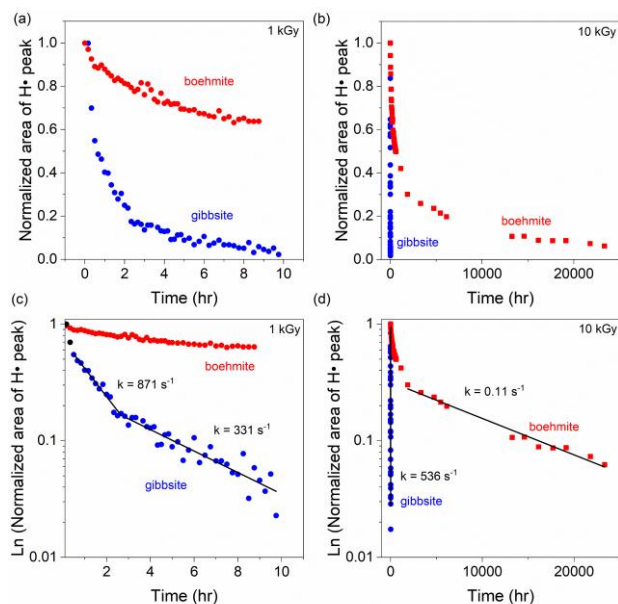


Figure 4. Decay of the integrated H atom peak intensity for (■) boehmite and (●) gibbsite at (a) 1 kGy and (b) 10 kGy. Plots of the Ln of the integrated H atom peak intensity for (c) 1 kGy and (d) 10 kGy showing the regions of first order decays.

a slower rate of diffusion and subsequent recombination in boehmite. At 10 kGy, the concentration (spin density) of H atoms obtained from the integrated peaks was found to be almost six times greater in boehmite than in Cl-gibbsite ($1.7 \cdot 10^{13}$ spins/ mm^3 vs $2.7 \cdot 10^{12}$ spins/ mm^3), suggesting that the secondary reactions that consume H atoms are faster in gibbsite, and that the crystalline structure of boehmite allows for more efficient stabilization of H atoms. Figs. 4(a) and 4(b) show the decay of H atoms in both materials with initial doses of 1 and 10 kGy, respectively. H atoms in Cl-gibbsite decay quickly and 10 hours after irradiation almost no H atoms are detected. About 80% of H atoms decayed in the first two hours after exposure, regardless of the total dose. Irradiation at 55 Gy/min took considerable time, about 20 minutes for 1 kGy and 3 hours for 10 kGy of gamma radiation dose, so that only a steady-state concentration of radicals is detected with EPR. Logarithmic plots of the decays are given in Fig 4(c) and 4(d) for doses of 1 kGy and 10 kGy, respectively. H atom decay at the very short times do not show first or second order kinetics in either gibbsite or boehmite. The decay process may include H atom recombination to produce H_2 , and likely involves a complicated combination of transient species. At longer times, first order decay kinetics are observed for both boehmite and Cl-gibbsite. Cl-gibbsite reaches this limit within about 10 hours while boehmite requires thousands of hours. However, the limiting decay rates are very different, with a rate constant of $331 s^{-1}$ for Cl-gibbsite and $0.11 s^{-1}$ for boehmite. These long-time limiting processes are probably due to the release of H atoms from their trapped sites with possible diffusion to the surface or reformation of hydroxyl groups.

These results show that Cl-gibbsite has a very limited ability to stabilize H atoms in its structure compared to boehmite. The long-time results for both boehmite and Cl-gibbsite irradiated with 1 kGy or 10 kGy can be fit with first-order decay kinetics, suggesting that, by the time of measurement, the decay depends only on the residual concentration of H atoms. The whole decay curve collected for both boehmite and Cl-gibbsite irradiated to 1 or 10 kGy could not be fit with a single decay model, suggesting that different processes are involved at different times. Thus, EPR studies show that the elimination of a scavenging NO_3^- impurity allows the radiolytic formation and stabilization of H atoms in Cl-gibbsite; however, the radicals recombine and react much faster in gibbsite than in boehmite.

Conclusions

Radiolytic species generated in the radiolysis of gibbsite nanoplatelets depend on the residual ions trapped in the particles from the precursor material used in the synthesis. Nitrate ions are great scavengers of free electrons generated in radiolysis. When these ions are present in gibbsite, they compete with hydroxyl sites for electrons to affect H atom formation or trapping. Nitrate-free material containing residual chloride can trap H atoms; however, the concentration of H atoms decreases rapidly with time compared to H atom decay in boehmite. This rapid decay suggests that trapped H atoms in gibbsite are less stable than in boehmite. One possible

explanation is that the layered structure of boehmite is a better trap for H atoms than gibbsite. The nature of the oxygen species produced in radiolysis seems to not be affected by the residual ions present in gibbsite, and probably boehmite. Impurities in gibbsite and boehmite may affect the H₂ capabilities of the solids in radiolysis.

Author Contributions

Hanna Hlushko contributed to the writing of the original draft, visualization, investigation, formal analysis, data curation, and conceptualization. Alejandro Ramos Ballesteros contributed to the investigation, formal analysis and conceptualization. Jay LaVerne contributed to conceptualization, funding acquisition, project administration, and supervision. Ping Chen and Xin Zhang contributed to the investigation by synthesising gibbsite particles. Kevin Rosso contributed by project administration. Carolyn Pearce contributed by funding acquisition, project administration. All authors contributed to writing, review and editing.

Conflicts of interest

There are no conflicts to declare.

Acknowledgments

This research was supported by Interfacial Dynamics in Radioactive Environment and Materials (IDREAM), an Energy Research Center funded by the U.S. Department of Energy, Office of Science, Basic Energy Sciences (FWP 68932). We thank Kiva Ford for glasswork, the Materials Characterization Facility at Notre Dame for providing access to TGA, pXRD, and XPS, the Notre Dame Integrated Imaging Facility for SEM analysis, and Prof. Ian Carmichael for access to the facilities of the Notre Dame Radiation Laboratory, which is supported by the Division of Chemical Sciences, Geosciences and Biosciences, Basic Energy Sciences, Office of Science, United States Department of Energy through grant number DE-FC02-04ER15533. This contribution is NDRL-5414 from the Notre Dame Radiation Laboratory.

References

- W. J. Deutsch, K. J. Cantrell, K. M. Krupka, M. L. Lindberg, and R. J. Serne, *Appl. Geochem.* **26** (9-10), 1681 (2011); J. S. Page, J. G. Reynolds, G. A. Cooke, and B. E. Wells, *J. Hazard. Mater.* **384**, 5 (2020).
- R. A. Peterson, E. C. Buck, J. Chun, R. C. Daniel, D. L. Herting, E. S. Ilton, G. J. Lumetta, and S. B. Clark, *Environ. Sci. Technol.* **52** (2), 381 (2018).
- J. G. Reynolds, G. A. Cooke, D. L. Herting, and R. W. Warrant, *J. Hazard. Mater.* **209**, 186 (2012); H. A. Colburn and R. A. Peterson, *Environ. Prog. Sustain. Energy* **40** (1), 12 (2021).
- J. A. Kaddissy, S. Esnouf, D. Saffre, and J. P. Renault, *Int. J. Hydrog. Energy* **44** (7), 3737 (2019).
- J. A. LaVerne and P. L. Huestis, *J. Phys. Chem. C* **123** (34), 21005 (2019).
- Z. M. Wang, E. D. Walter, M. Sassi, X. Zhang, H. L. Zhang, X. H. S. Li, Y. Chen, W. W. Cui, A. Tuladhar, Z. Chase, A. D. Winkelman, H. F. Wang, C. I. Pearce, S. B. Clark, and K. M. Rosso, *J. Hazard. Mater.* **398**, 11 (2020).
- E. T. Nienhuis, T. R. Graham, N. L. D'Annunzio, M. I. Kowalska, J. A. LaVerne, T. M. Orlando, J. G. Reynolds, D. M. Camaioni, K. M. Rosso, C. I. Pearce, and E. D. Walter, *Journal of Chemical Physics* **158** (22), 14 (2023).
- E. Briley, P. Huestis, X. Zhang, K. M. Rosso, and J. A. LaVerne, *Mater. Chem. Phys.* **271**, 8 (2021).
- J. A. Kaddissy, S. Esnouf, D. Durand, D. Saffre, E. Foy, and J. P. Renault, *J. Phys. Chem. C* **121** (11), 6365 (2017).
- Z. Z. Shen, E. S. Ilton, M. P. Prange, C. J. Mundy, and S. N. Kerisit, *J. Phys. Chem. C* **122** (50), 28990 (2018).
- X. Zhang, X.-W. Zhang, T. R. Graham, C. I. Pearce, B. L. Mehdi, A. N'Diaye, S. Kerisit, N. D. Browning, S. B. Clark, and K. M. Rosso, *Cryst. Growth Des.* **17**, 6801 (2017); X. Zhang, P. L. Huestis, C. I. Pearce, J. Z. Hu, K. Page, L. M. Anovitz, A. B. Aleksandrov, M. P. Prange, S. Kerisit, M. E. Bowden, W. W. Cui, Z. M. Wang, N. R. Jaegers, T. R. Graham, M. Dembowski, H. W. Wang, J. Liu, A. T. N'Diaye, M. Bleuel, D. F. R. Mildner, T. M. Orlando, G. A. Kimmel, J. A. La Verne, S. B. Clark, and K. M. Rosso, *ACS Appl. Nano Mater.* **1** (12), 7115 (2018).
- A. Malki, Z. Mekhalif, S. Detriche, G. Fonder, A. Bournaza, and A. Djelloul, *J. Solid State Chem.* **215**, 8 (2014).
- E. Balan, M. Lazzeri, G. Morin, and F. Mauri, *Am. Miner.* **91** (1), 115 (2006).
- D. J. Goebbert, E. Garand, T. Wende, R. Bergmann, G. Meijer, K. R. Asmis, and D. M. Neumark, *J. Phys. Chem. A* **113** (26), 7584 (2009).
- M. Sassi, E. D. Walter, O. Qafoku, K. M. Rosso, and Z. M. Wang, *J. Phys. Chem. C* **124** (40), 22185 (2020).
- P. L. Huestis, T. R. Graham, S. T. Mergelsberg, and J. A. LaVerne, *Thermochim. Acta* **689**, 9 (2020).
- V. Seeman, A. Lushchik, E. Shablonin, G. Prieditis, D. Gryaznov, A. Platonenko, E. A. Kotomin, and A. I. Popov, *Sci Rep* **10** (1), 14 (2020).